Monolithically Integrated High-Gain and High-Sensitive Photoreceivers with Tunable Filtering Functions for Subcarrier Multiplexed Optical/Microwave Systems

Hideki Kamitsuna, *Member, IEEE*

Abstract—**This paper proposes monolithically integrated photoreceivers with tunable filtering functions using HBT-compatible HPT's for band-limited microwave subcarrier multiplexed transmission and optical/microwave signal processing systems. The filter photoreceiver, which consists of the HPT with a positive feedback LC resonance circuit and a Q-damping resistor, realizes the high quality factor (Q-factor) of 37.7 with the photo-response peak frequency of 13.6 GHz. Furthermore, it yields not only 24.1 dB and 16.2 dB higher gain but also over 7.5 dB and 3.5 dB improvement in sensitivity at 13.6 GHz without any spurious oscillation, in comparison with a standard photodiode and a discrete HPT, respectively. The tuner photoreceiver is constructed based on the filter photoreceiver. By adapting the HBT-compatible varactor diode in the resonance circuit, we realize tunable filtering functions, i.e., a very-wide photo-response peak frequency tuning range of 11.0–14.6 GHz with a Q-factor of over 20.2. The chip size is as small as 1.0 mm × 0.75 mm. The developed photoreceivers promise to realize compact, cost-effective hardware for subcarrier multiplexed optical/microwave or /millimeter-wave systems.**

I. Introduction

MMIC compatible photodetectors are very attractive in realizing very small, cost-effective photoreceivers for microwave transmission via optical subcarrier systems and for optical/microwave signal processing systems. MMIC compatible photodetectors such as three-terminal HPT's and HEMT's can realize highly-sensitive photodetectors due to their internal gain [1] and optoelectronic mixers [2] due to their large nonlinearity. Among these photodetectors, three-terminal HPT's are the most promising high-performance photodetectors. This is because they offer, unlike MESFET's or HEMT's, easy photo-coupling due to their vertical device structures and photodetection gain up to the millimeter-wave frequencies by using the same epitaxial layer of the ultra-high-frequency HBT's [3]. Although the photodetection performances of discrete HPT's have been reported [3]–[5], no work has been done with respect to realizing high-performance functional photoreceivers operating at microwave frequencies in an integrated circuit fashion. Since three-terminal HPT's offer good RF performance for both microwave amplification and photodetection and are easily integrated with high-frequency active and passive components, integrated circuit technologies are expected to further improve the performance and realize additional functions.

The photoreceiver performance for band-limited systems should be optimum at the frequency band of interest, unlike the ultra-wideband characteristics of photoreceivers for high-bit-rate digital transmission. In addition, since most systems employ the subcarrier multiplexed transmission [6], a filter function is also required if the receiver is to select only the desired subcarrier signal. Furthermore, a frequency tuning function must be added to realize a cost-effective integrated photoreceiver applicable to systems using different frequency bands. This is also very beneficial for temperature and process-fluctuation compensation.

This paper presents monolithically integrated photoreceivers with tunable filtering functions based on HBT-compatible three-terminal HPT's [4] for such band-limited optical/microwave systems. First, the filter photoreceiver, which consists of the HPT with positive feedback LC resonance circuit and Q-damping resistor, is discussed. Second, the tuner photoreceiver, by adopting HBT-compatible varactor diodes in the filter photoreceiver, is presented. They fully utilize the combination of ultra-high-frequency HPT's with positive feedback circuits. The performance of the proposed photoreceiver is compared with that of the discrete HPT under both Tr- and PD-mode bias condition [3], [4], since discrete HPT's yield good response under both Tr- and PD-mode operation [3], [4] and high-sensitive performances under Tr-mode operation [4]. X- and Ku-band monolithic photoreceivers using AlGaAs/GaAs HPT/HBT's are designed and fabricated. Excellent performance, i.e., high-gain with (tunable) filtering functions and high-sensitivity is demonstrated in good agreement with the simulated results.

II. Functional Photoreceivers for Band-Limited Systems

The photoreceiver for microwave subcarrier multiplexed transmission via an optical fiber [6] includes, as a minimum,

Manuscript received January 16, 1995; revised April 1, 1995.

The author is with NTT Wireless Systems Laboratories, Kanagawa 238-03, Japan.

IEEE Log Number 9413689.

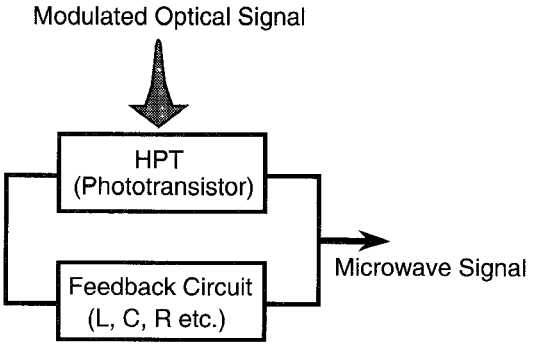

Fig. 1. Functional photoreceiver circuit configuration consists of the phototransistor such as HPT's and the positive feedback circuit.

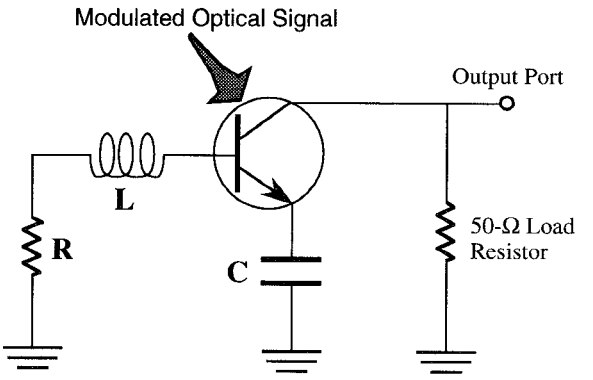

Fig. 2. Circuit schematic of the proposed filter photoreceiver.

a photodetector, a microwave amplifier and a filter. This configuration is nearly identical for optical/microwave signal processing systems using optical self-heterodyning techniques which generate microwave signals at the photodetector [7]. In both systems, the photoreceiver performance should be optimum at the frequency band of interest. The difference in requirements lies in the filter characteristics. A higher Q-factor, in addition to the frequency tuning function, is required by the former system.

To realize compact, cost-effective, and high-performance photoreceivers for such purposes, the functional photoreceiver circuit configuration that consists of phototransistors such as HPT's and positive feedback circuits is proposed as shown in Fig. 1. The proposed circuit configuration allows us not only to increase photodetection signal levels but also to realize functions such as filtering by adapting suitable positive feedback resonance circuits. Although, a few studies of photoreceivers for microwave subcarrier transmission utilizing a "resonance" phenomena have been reported [8], their concept and performance are quite different from the photoreceiver proposed here. The proposed photoreceiver configuration realizes functional phototransistor circuits by adapting the positive feedback circuit to the phototransistor. Combining ultra-high-frequency phototransistors with positive feedback circuits enables us to realize a high Q-factor filtering characteristic up to micro- or millimeter-wave frequencies unlike the utilization of "resonance" only.

III. Filter Photoreceiver

A. Configuration and Design

The proposed filter photoreceiver, shown in Fig. 2, is one concrete example of the functional photoreceiver circuit. This circuit is based on the common-emitter series feedback oscillator scheme [9] with Q-damping resistor R. This photoreceiver circuit allows us to achieve high-gain with filtering functions due to the positive feedback LC resonance circuit; unnecessary spurious oscillation is suppressed by the Q-damping resistor R. All circuit parameters were designed for 13-GHz-band subcarrier detection.

First, stable photoreceiver operation as a function of the Q-damping resistance R was evaluated. Fig. 3 shows the simulated reflection coefficients (magnitude and angle) of the

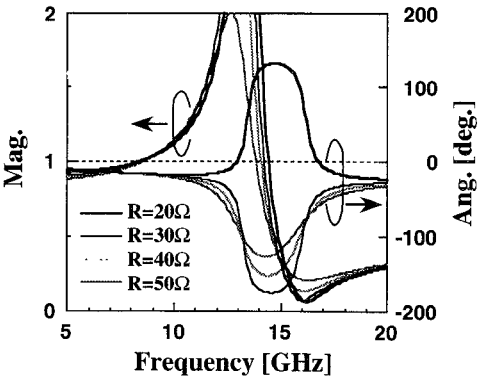

Fig. 3. Simulated reflection coefficients (magnitude and phase) of the filter photoreceiver circuit seen from the output port with the Q-damping resistances R of 20, 30, 40, and 50 Ω.

filter photoreceiver circuit seen from the output port. Reflection magnitudes of over unity, one condition requirement for oscillation [10], were observed even if $R = 50\,\Omega$ in the frequency range of 8–15 GHz. However, the other requirement, a reflection phase of zero [10], is avoided when R exceeds 30 Ω. Therefore, we can expect a significant increase in the photodetection gain in the vicinity of 13 GHz and improved receiver sensitivity without unnecessary self-oscillation signals with Q-damping resistances over 30 Ω.

Fig. 4 shows simulated photo-responses of the filter photoreceivers with the Q-damping resistances R of 30, 40, and 50 Ω. The simulated results of the discrete common-emitter HPT is also plotted. In the simulation, the equivalent circuit derived from the measured S-parameters and the current source model were utilized for the HPT part and the optical/RF conversion part, respectively [3]. The emitter size and the emitter/base electrode gap for photo-coupling of the HPT utilized in the simulation were 2 μm $\times$ 10 μm and 3 μm, respectively [4]. The current gain cut-off frequency (f_T) and maximum oscillation frequency ($f_{\max}$) were 44 GHz and 40 GHz, respectively. All the filter photoreceivers yield over 10 dB gain against the discrete HPT in the vicinity of 13 GHz. In addition, filtering functions with decreasing photo-response in the out-of-13-GHz-band was achieved. When R increases, both the gain and the Q-factor for the filter photoreceiver decrease since the Q-factor of the resonance circuit decreases. In other words, it is possible to design the photoreceiver bandwidth in accordance with the transmitted signal bandwidth.

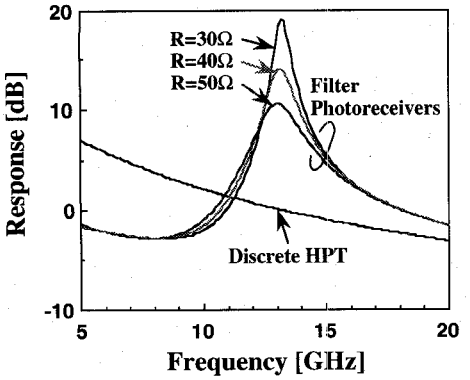

Fig. 4. Simulated relative frequency responses of the filter photoreceivers with the Q-damping resistances R of 30, 40, and 50 Ω. The simulated result of the discrete HPT is also plotted.

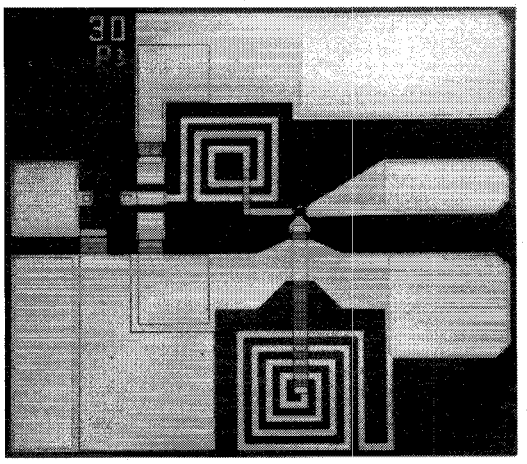

Fig. 5. Photomicrograph of the fabricated filter photoreceiver with R of 30 Ω. Chip size: 0.71 mm × 0.62 mm.

B. Experimental Results

1) Frequency Response: A monolithically integrated photoreceiver was fabricated with the HBT-compatible AlGaAs/GaAs HPT, a spiral inductor, MIM capacitors and resistors. Filter photoreceiver circuits with Q-damping resistances R of 30, 40, and 50 Ω were tested. Fig. 5 shows a photomicrograph of the fabricated filter photoreceiver with R of 30 Ω. The chip size of each photoreceiver was 0.71 mm × 0.62 mm.

A modified electrooptic on-wafer RF probe station [1], a 0.83-μm LD, an $LiNbO_3$ external optical modulator (EOM: optical insertion loss of 9.2 dB, half-wave voltage (V_π) of 2 V and 3 dB-bandwidth of approximately 13 GHz), and a network analyzer were utilized to measure the frequency response. The optical spot diameter was approximately 10 μm. In the following figures, the link loss expresses the insertion loss measured by the network analyzer which includes the EOM's frequency response.

This paper compares the performance of the fabricated photoreceiver circuits with that of the discrete HPT [4]. Two bias conditions, i.e., normal three terminal transistor operation (Tr-mode, $V_{CE} = 2$ V, $I_C = 8$ mA) and PD-mode operation (V_{CB} =2 V, V_{BE} =0 V) [3], [4] were tested for the discrete HPT. The PD-mode allows us to utilize three terminal

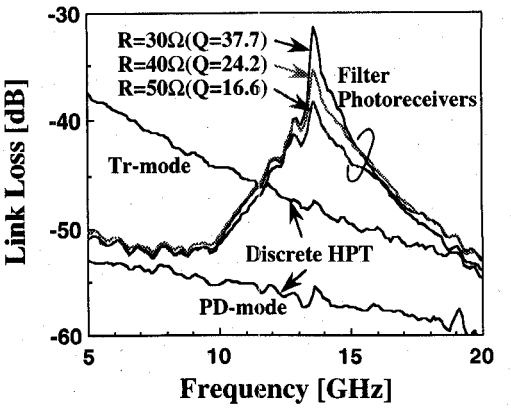

Fig. 6. Measured frequency responses (link losses) of the filter photoreceivers (Q-damping resistances R of 30, 40, and 50 Ω) and the discrete HPT. The averaged optical input power is 0.2 mW. The bias condition is set to $V_{CE} = 2$ V and $I_C = 8$ mA (Tr-mode). The PD-mode bias condition where $V_{CB} = 2$ V and $V_{BE} = 0$ V are also conducted for the discrete HPT.

HPT's as photodiodes and can be considered as the standard photodiode of the Tr-mode HPT [4].

Fig. 6 shows the measured frequency responses (link losses) of the three filter photoreceivers (Q-damping resistances R of 30, 40, and 50 Ω). That of the discrete HPT is also plotted for comparison. The averaged optical input power was 0.2 mW. The bias condition was $V_{CE} = 2$ V and $I_C = 8$ mA and no oscillation signal was observed for all filter photoreceiver circuits under both dark and illumination condition. The Q-factors for the filter photoreceivers were 37.7 ($R = 30\,\Omega$), 24.2 ($R = 40\,\Omega$) and 16.6 ($R = 50\,\Omega$). The ability to design the photoreceiver bandwidth was demonstrated to be in good agreement with the simulated results. Furthermore, the filter photoreceivers yield high-gain of 16.2 dB ($R = 30\,\Omega$), 12.1 dB ($R = 40\,\Omega$), and 9.2 dB ($R = 50\,\Omega$) compared to the discrete HPT (Tr-mode) at 13.6 GHz. The corresponding gains are 24.1 dB ($R = 30\,\Omega$), 20.0 dB ($R = 40\,\Omega$), and 17.1 dB ($R = 50\,\Omega$) against the photodiode with equal quantum efficiency (PD-mode HPT).

2) Noise Performance: Both the photo-detected subcarrier levels of C and the noise power density 1 MHz from the subcarrier frequency (N_0, dBm/Hz) were measured by changing the illuminated optical power with the optical attenuator. An external microwave amplifier (gain: 37.3 dB, NF: 5.9 dB, @13.5 GHz) was used to lower the noise floor of the spectrum analyzer. The noise performance was evaluated by the C/N_0 ratio. The filter photoreceiver with the Q-damping resistance R of 30 Ω and the discrete HPT were compared. Both Tr- and PD-mode bias conditions were examined for the discrete HPT. The RF power supplied to the EOM was 0 dBm.

Fig. 7 shows the measured C/N_0 performances for the filter photoreceiver (R =30 Ω) and the discrete HPT (Tr- and PD-modes) at the RF (subcarrier) frequency of 13.6 GHz. The filter photoreceiver yields a C/N_0 improvement of over 5.1 dB and 12.1 dB against the discrete HPT (Tr- and PD-mode), respectively when the optical input power is under −13.9 dBm (receiver noise is dominant). For example, when the C/N_0 of 90 dB is required, the filter photoreceiver offers sensitivity improvements of 3.5 dB and 7.5 dB over

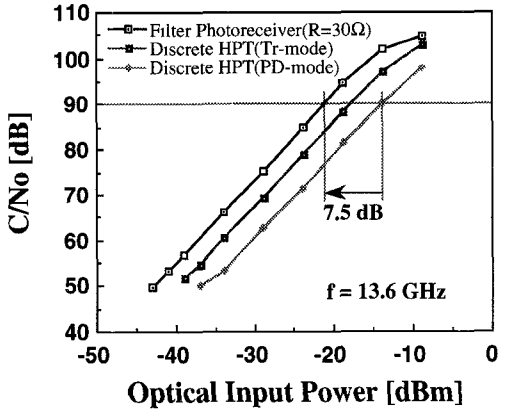

Fig. 7. Measured C/N_0 performances of the filter photoreceiver ($R = 30\,\Omega$) and the discrete HPT (Tr- and PD-modes). The RF (subcarrier) frequency is 13.6 GHz and the RF power supplied to the EOM is 0 dBm.

the discrete HPT (Tr-mode) and the photodiode with equal quantum efficiency (PD-mode HPT), respectively. Since the C/N_0 curve saturation is mostly determined by the relative intensity noise of the laser diode, occurring the saturation in the lower optical input power means the low noise performance of the filter photoreceiver.

IV. Tuner Photoreceiver

A. Configuration and Design

Placing variable reactance elements into the positive feedback LC resonance circuit in the filter photoreceiver realizes frequency tuning. Fig. 8 shows the circuit schematic of the proposed tuner photoreceiver. This circuit places an HBT-compatible varactor diode [9] in the LC resonance circuit and integrates an HBT buffer amplifier to realize stable operation over a wide frequency range. The Q-damping resistance R is set to $60\,\Omega$ to giving sufficient margin for suppressing self-oscillation and changing HPT structures discussed in the previous section. The HBT and the HPT use the same epitaxial layer structure; the HPT uses a different electrode structure for better photo-coupling [4]. The varactor diode consists of the base/collector layer of the HBT with the emitter layer removed [9]. Therefore, the HPT, HBT, and the varactor diode are HBT MMIC process compatible. The emitter size and the photo-coupling window size at the emitter electrode of the HPT were 6 μm $\times$ 9 μm and 5 μm $\times$ 6 μm, respectively [4]. The current gain cut-off frequency (f_T) and maximum oscillation frequency ($f_{\max}$) of the HPT were 46 GHz and 67 GHz, respectively. The f_T and $f_{\max}$ of an HBT (emitter size of 2 μm $\times$ 10 μm) utilized in the photoreceiver were 58 GHz and 78 GHz, respectively. Although such excellent microwave performances of both the HPT and the HBT are enough for millimeter-wave applications, this paper describes and demonstrates X- and Ku-bands photoreceivers. Millimeter-wave photoreceivers will be demonstrated in the near future.

Fig. 9 shows the capacitance variation of the HBT-compatible varactor diode determined from the measured S-parameters as a function of the cathode (collector) to anode (base) voltage (V_{cb}). The capacitance variation ratios

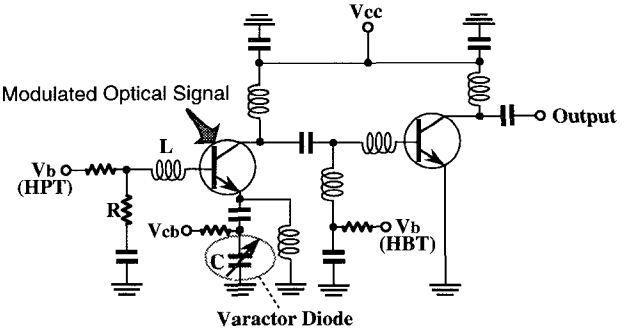

Fig. 8. Circuit schematic of the proposed tuner photoreceiver.

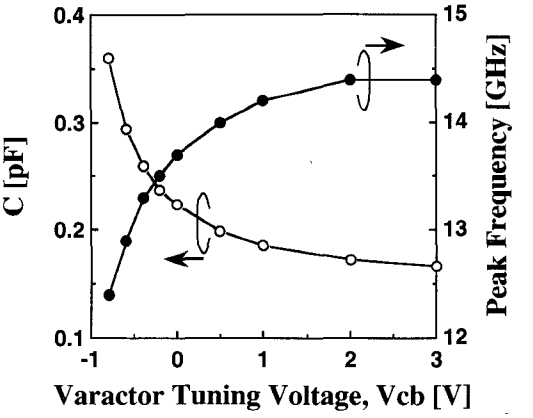

Fig. 9. Capacitance variable characteristics of the HBT-compatible varactor diode and the simulated photo-response peak frequency of the tuner photoreceiver as a function of the varactor tuning voltage, V_{cb}.

were 1:1.34 and 1:2.16 for the V_{cb} ranges of 0–3 V and −0.8–3 V, respectively. This varactor diode can operate under the forward junction bias condition ($V_{cb} < 0$ V) because the photodetector outputs are extremely small signal levels (typically less than −20 dBm). Therefore, the very wide capacitance variation range of over 1:2.16 under the forward bias condition approaching the forward breakdown voltage ($V_{cb} \sim -1.1$ V) can be fully utilized for the photoreceiver application. Fig. 9 also shows the simulated frequency tuning performance of the tuner photoreceiver (Fig. 8), using the capacitance value of the varactor diode at each V_{cb}. The extreme large peak frequency tuning range of 12.4–14.4 GHz is predicted by the varactor tuning voltage V_{cb} of −0.8–+3 V.

B. Experimental Results

Fig. 10 shows a photomicrograph of the fabricated tuner photoreceiver. This circuit pattern layout is based on the lumped uniplanar MMIC structure [11] to minimize the chip size. The chip size is 1.0 mm $\times$ 0.75 mm. Fig. 11 shows the measured frequency responses (link losses) of the tuner photoreceiver under varactor tuning voltages (V_{cb}) of −1, −0.9, −0.8, −0.6, −0.4, 0, +1, and +3 V. Fig. 12 shows the measured photo-response peak frequency and the Q-factor as functions of the V_{cb}. The remarkable wideband frequency tuning range from 11.0 GHz ($V_{cb} = -1$ V) to 14.6 GHz ($V_{cb} = +3$ V) is in good agreement with the simulated results. Since the varactor diode experiences very low signal powers,

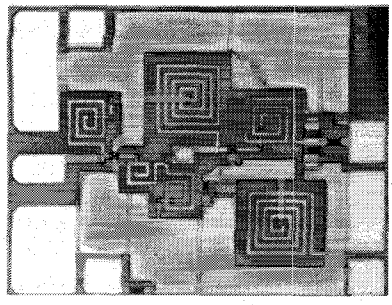

Fig. 10. Photomicrograph of the fabricated tuner photoreceiver. Chip size: 1.0 mm × 0.75 mm.

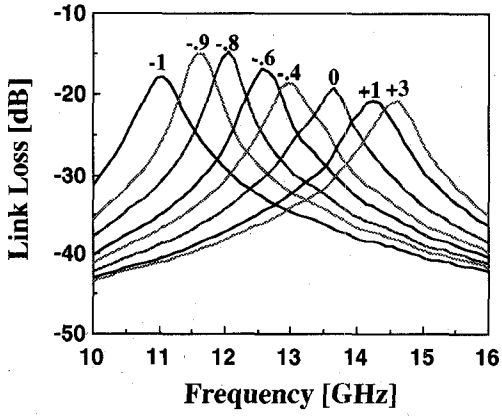

Fig. 11. Measured frequency responses (link losses) of the tuner photoreceiver under the varactor tuning voltage (V_{cb}) of -1, -0.9, -0.8, -0.6, -0.4, 0, $+1$, and $+3$ V. The averaged optical input power is 0.2 mW. The numerical values in the figure represent varactor tuning voltage, V_{cb}.

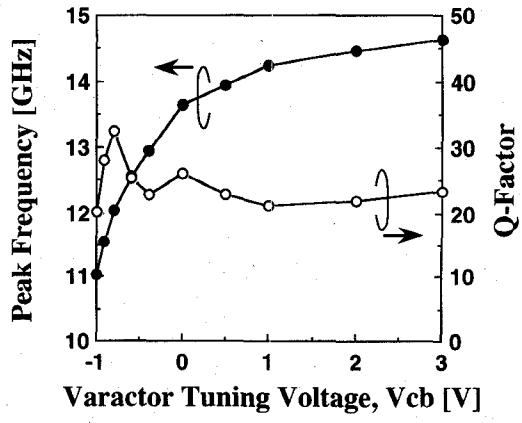

Fig. 12. Measured photo-response peak frequency and Q-factor as a function of the varactor tuning voltage, V_{cb}.

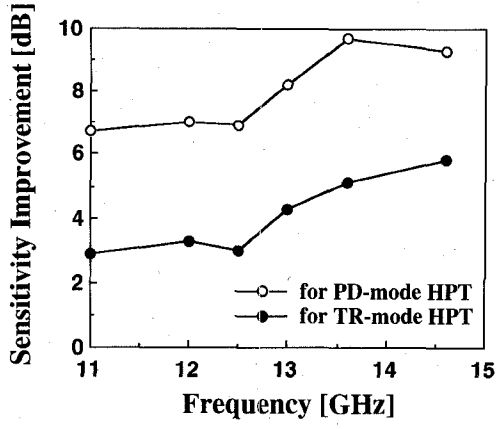

Fig. 13. Sensitivity improvement by the tuner photoreceiver against the discrete HPT (Tr- and PD-modes) in the RF (subcarrier) frequency range 11 to 14.6 GHz when the C/N_0 of 90 dB is required.

stable operation up to the vicinity of its forward breakdown voltage is achieved. Furthermore, the Q-factor of over 20.2 was achieved in this frequency range. Although the obtained Q-factors were slightly lower than the highest ones of the filter photoreceiver because $R = 60\,\Omega$, the Q-factor can be increased by decreasing the Q-damping resistance as shown in Fig. 6. The photo-response decrease as the tuning frequency increases (V_{cb} increases), shown in Fig. 11, is due to these data including the frequency response of the EOM. Therefore, almost flat photo-response over the wideband of 3 GHz has been achieved.

Fig. 13 shows the sensitivity improvement offered by the tuner photoreceiver against the discrete HPT (both Tr- and PD-modes) in the RF (subcarrier) frequency range of 11–14.6 GHz when achieving the C/N_0 of 90 dB. The varactor tuning voltage V_{cb} was adjusted to obtain the optimum photo-response peak at each subcarrier frequency. Receiver sensitivity improvements of over 2.9 dB and 6.7 dB were achieved against the discrete HPT (Tr-mode) and the photodiode with equal quantum efficiency (PD-mode HPT), respectively.

V. Conclusion

This paper has presented monolithically integrated high-gain and high-sensitive photoreceivers with tunable filtering functions for band-limited microwave subcarrier transmission and optical/microwave signal processing systems. Functional HPT photoreceivers operating at microwave frequencies have been successfully demonstrated for the first time. The wide-tuning frequency ability is very effective in realizing a cost-effective photoreceiver since it enables us to utilize the same integrated photoreceiver in many systems operating at different frequency bands. This is also very beneficial for temperature and process-fluctuation compensation. Proposed photoreceivers offer a very wide application frequency range from UHF to millimeter-waves by changing only the circuit parameters of the positive feedback LC resonance circuit, since they are designed and fabricated using mature MMIC technologies. Although the obtained Q-factors are insufficient for filtering the desired signal from a dense subcarrier multiplexed allocation, the proposed photoreceiver can simplify the receiver configuration in subcarrier multiplexed optical/microwave systems. This is because it reduces the demand for subsequent amplifiers and filters. Furthermore, it can be successfully utilized in optically-fed multibeam phased array applications [7] in which all subcarrier signals within a particular bandwidth must be detected. The photoreceiver circuit will demonstrate excellent performance for middle/long distance optical transmission systems which utilize 1.3- or 1.55-μm band if realized using InP based HPT/HBT's [3].

ACKNOWLEDGMENT

The author would like to thank Dr. Y. Yamauchi of NTT LSI Laboratories for his helpful assistance throughout this work. The author also would like to thank Dr. K. Kohiyama, Dr. S. Samejima, Dr. H. Ogawa, Dr. K. Hirata, and Dr. T. Ishibashi for their continuous support and encouragement.

REFERENCES

[1] H. Ogawa, S. Banba, E. Suematsu, H. Kamitsuna, and D. Polifko, "A comparison of noise performance between a PIN diode and MMIC HEMT and HBT optical receivers." in *1993 IEEE MTT-S Int. Microwave Symp. Dig.*, June 1993, pp. 225–228.

[2] H. Kamitsuna and H. Ogawa, "Monolithic image-rejection optoelectronic up-converters that employ the MMIC process," *IEEE Trans. Microwave Theory Tech.*, vol. 41, pp. 2323–2329, Dec. 1993.

[3] H. Kamitsuna, Y. Matsuoka, S. Yamahata, H. Nakajima, and H. Ogawa, "Photodetection characteristics of InP/InGaAs HBT's and their process compatible pin-photodiodes," in *19th Int. Conf. Infrared Millimeter Waves Dig.*, Oct. 1994, pp. 325–326.

[4] H. Kamitsuna, Y. Yamauchi, and H. Ogawa, "Photodetection characteristics of AlGaAs/GaAs HBT's with various photo-coupling electrode structures," in *1994 Asia-Pacific Microwave Conf. Proc.*, Dec. 1994, pp. 1159–1162.

[5] E. Suematsu and H. Ogawa, "Frequency response of HBT's as photodetectors," *IEEE Microwave Guided Wave Lett.*, vol. 3, pp. 217–218, July 1993.

[6] R. Olshansky, V. A. Lanzisera, and P M Hill, "Subcarrier multiplexed lightwave systems for broadband distribution," *J. Lightwave Technol.*, vol. 7, pp. 1329–1341, Sept. 1989.

[7] K. Horikawa, Y. Nakasuga, and H. Ogawa, "Self-heterodyning optical beam forming network for multibeam active phased array antenna," in *The 24th European Microwave Conf. Proc.*, Sept. 1994, pp. 1673–1678.

[8] T. E. Darcie, B. L. Kasper, J. R. Talman, and C. A. Burrus, Jr., "Resonant p-i-n-FET receivers for lightwave subcarrier systems," *J. Lightwave Technol.*, vol. 6, pp. 582–589, Apr. 1988.

[9] Y. Yamauchi, H. Kamitsuna, M. Nakatsugawa, H. Ito, M. Muraguchi, and K. Osafune, "A 15-GHz monolithic low-phase-noise VCO using AlGaAs/GaAs HBT technology," *IEEE J. Solid-State Circuits*, vol. 27, pp. 1444–1447, Oct. 1992

[10] R. S. Pengelly, "Microwave field-effect transistors—Theory, design, and applications," in *Research Studies Press*, 1982, pp. 275–2278.

[11] T. Hirota and M. Muraguchi, "A *K*-band single-chip transmitter," in *1990 IEEE GaAs IC Symp. Dig.*, Oct. 1990, pp. 275–278.

Hideki Kamitsuna (M'91), photograph and biography not available at the time of publication.